European Heart Journal – Cardiovascular Imaging (2013) **14**, 797–804
doi:10.1093/ehjci/jes273

Wall shear stress and flow patterns in the ascending aorta in patients with bicuspid aortic valves differ significantly from tricuspid aortic valves: a prospective study

Christian Meierhofer[1]*, Eike Philipp Schneider[2], Christine Lyko[1], Andrea Hutter[2], Stefan Martinoff[3], Michael Markl[4,5], Alfred Hager[1], John Hess[1], Heiko Stern[1], and Sohrab Fratz[1]

[1]Department of Pediatric Cardiology and Congenital Heart Disease; [2]Department of Cardiovascular Surgery; [3]Division of Radiology, Deutsches Herzzentrum München, Technische Universität München (TUM), Lazarettstrasse 36, 80636 Munich, Germany; [4]Department of Radiology, Feinberg School of Medicine, Northwestern University, Chicago, IL, USA; and [5]Department of Biomedical Engineering, McCormick School of Engineering, Northwestern University, Chicago, IL, USA

Received 26 October 2012; accepted after revision 5 November 2012; online publish-ahead-of-print 9 December 2012

Aims We compared flow and wall shear stress (WSS) patterns in the ascending aorta of individuals with either bicuspid aortic valve (BAV) or tricuspid aortic valve (TAV) using four-dimensional cardiovascular magnetic resonance (4D-CMR). BAV are known to be associated with dilation and dissection of the ascending aorta. However, the cause of vessel disease in patients with BAVs is unknown. Inborn connective tissue disease and also dilation secondary to increased WSS because of altered blood flow patterns in the ascending aorta are discussed as causes for dilation of the aorta. WSS can be estimated non-invasively by 4D-CMR.

Methods and results Eighteen, otherwise, healthy individuals with functionally normal BAVs were compared prospectively with an age- and sex-matched control group of healthy individuals with TAV. Blood flow data were obtained by 4D-CMR visualization and WSS was calculated with specific software tools. Eighty-five per cent of the individuals with BAVs showed a high-grade helical flow pattern in the ascending aorta compared with 6% of the individuals with TAV. WSS in the ascending aorta was significantly altered in individuals with BAVs compared with TAV.

Conclusion WSS and flow patterns in the ascending aorta in patients with BAVs without concomitant valve or vessel disease are significantly different compared with TAV. The significantly higher shear forces may have an impact on the development of aortic dilation in patients with BAVs.

Keywords Bicuspid aortic valve • Blood flow • Wall shear stress • Cardiovascular magnetic resonance imaging

Introduction

A bicuspid aortic valve (BAV) is the most common congenital heart defect.[1–4] Most of the patients with BAV are asymptomatic and complications such as aortic dissection are rare in children, but symptoms may develop in adulthood.[5] An association between congenital BAV and aortic wall alterations such as aortic dilatation and dissection is well known.[6–11] Aortic dilatation, even in individuals with normally functioning aortic valves, occurs at all levels of the aorta, but usually targets the ascending aorta.[12] However, the cause of the dilation of the ascending aorta in BAV remains unknown and is the topic of two opposing theories.[4,13] The first theory argues that an inborn disorder of vascular connective tissue, formerly misleadingly named *cystic media necrosis*,[14] of the ascending aortic wall might be the reason for its weakness leading to dilation, dissection, or rupture.[4] A second theory favours altered haemodynamic forces on the aortic wall caused by the BAV causing a secondary disorder of vascular connective

* Corresponding author. Tel: +49 89 1218 0; fax: +49 89 1218 3013, Email: meierhofer@dhm.mhn.de

tissue leading to aortic dilation in individuals with BAV.[13] Complex flow patterns in the aorta can now be visualized non-invasively by four-dimensional (4D) cardiovascular magnetic resonance (CMR). Several studies showed a complex helical flow pattern in patients with BAV and aneurysm formation using 4D-CMR although the cause–effect relationship remains unclear because most of these patients had additional cardiovascular diseases such as coarctation of the aorta or Fallot's tetralogy.[15,16]

Force and direction of wall shear stress (WSS) can now be estimated at any level of the aortic vessel wall by using these 4D-CMR data sets.[17–22]

Therefore, the purpose of this study was to compare flow patterns and WSS in the ascending aorta in individuals without any other concomitant cardiovascular disease other than BAV or tricuspid aortic valve (TAV). We investigated *in vivo* flow patterns and WSS in the ascending aorta in two prospective age- and sex-matched groups with either BAV or TAV morphology by 4D-CMR.

Methods

Bicuspid aortic valve study group

Prospectively, 989 patients with the diagnosis BAV were identified in the hospital's database out of a total of 32 794 patients with congenital heart disease. Out of 989 selected patients, 18 individuals met the final inclusion criteria: age >7 years, no existing or past cardiovascular disease other than BAV, no arterial hypertension, no connective tissue disorders in the medical history or thorax deformations, no medication, a flow velocity through the aortic valve of <2.5 m/s by echocardiography, no moderate or severe aortic valve regurgitation by echocardiography, a diameter of the ascending aorta <4.5 cm in adults and <2.2 cm/m^2 in children, no contraindications to CMR imaging.

The inclusion criteria were chosen to form a homogeneous and strict study group of individuals with only BAV and as few confounding factors as possible effecting flow in the ascending aorta. We used the aforementioned cut-off values for aortic valve stenosis and regurgitation and the diameter of the ascending aorta as inclusion criteria because these values are considered as clinically significant in current guidelines.[4,5,23]

Tricuspid aortic valve control group

Eighteen healthy volunteers (eight females) were prospectively matched to the BAV study group to serve as the TAV control group. Valve morphology was evaluated and confirmed during the CMR study by cine studies. The TAV control group was matched by sex and age (± 2 years).

Cardiovascular magnetic resonance

A standard cardiac 1.5 Tesla MRI scanner (MAGNETOM Avanto®, version software VB15, Siemens Healthcare, Erlangen, Germany) with a standard 12-channel body-coil was used for the CMR study.

Aortic valve morphology

Through the aortic valve a double-oblique orientated retrospectively ECG-triggered multi-phased steady-state free precession sequence was used for leaflet morphology (slice thickness of 4, 5, or 6 mm depending on the body weight, acquisition matrix 192 × 192, 25 phases/cardiac cycle). Leaflet morphology was classified as previously described.[24] In brief, BAV type 1 was classified as fusion of the right and left coronary cusp, BAV type 2 as fusion of the right and non-coronary cusp. There was no case with fusion of the left and non-coronary cusp (BAV type 3).

Four-dimensional cardiovascular magnetic resonance

The aortic blood flow was visualized using a time-resolved three-dimensional phase-contrast sequence with three-directional velocity encoding as previously described.[18] The flow-sensitive 4D sequence was triggered retrospectively by ECG. No contrast agent was used. Respiration was compensated by navigator gating. All data were measured in a sagittal-oblique volume that included the entire left ventricular outflow tract as well as the ascending aorta, the aortic arch with the aortic branches and the thoracic descending aorta. The measurements yielded in a three-dimensional volume coverage with a spatial resolution of 2.1 × 1.7 × 2.5 mm^3; TR 39.2 ms; TE 2.417 ms; FOV 240 × 320 mm; field of view phase 75%; velocity encoding Vx, Vy, and Vz 200–230 cm/s; layer thickness 2.5 mm; flip angle 8°–10°; band width 455 Hz/pixel. With dedicated software tools based on Matlab® (The MathWorks, Natick, MA, USA) DICOM data from 4D-CMR were converted for further processing and data underwent semi-automated noise filtering and eddy-current correction. The noise filtering, eddy-current correction, anti-aliasing, and deletion of static tissue were set to identical parameters in each case. For further enhancement of vascular regions with high flow and suppression of background signal, an additional time-independent phase-contrast-MR-angiography (PC-MRA) data set was generated by the squared sum of the individual 3D PC-MRA images (*Figure 1*).[18,25]

Blood flow pattern

The generated data sets were further processed by EnSight® software package (EnSight®; CEI, Apex, NC, USA) as previously described (*Figure 1*).[18,19,21,22,25,26] Hereby, it was possible to generate 3D interactive anatomical images of the thoracic aorta. This allowed for 4D flow visualization with 3D streamlines and time-resolved 3D particle traces (EnLiten®; CEI, Apex, NC, USA) (*Figure 2*). For flow pattern evaluation, the display options of the visualized flow data were set to identical parameters in all cases.

All the 36 flow patterns in the ascending aorta of the 18 individuals of the BAV study group and of the 18 individuals of the TAV control group were graded in random order using a pre-defined grading scale in a blinded fashion by three investigators. The three investigators did not take part in visualization or processing of the data. Grade 0 was defined as linear flow in the ascending aorta, Grade 1 as a helical flow of <180°, Grade 2 as a helical flow of 180–360°, and Grade 3 as a helical flow of >360° (*Figure 3*). The number of observations by the three investigators for each grade of helical flow was added to a score.

Wall shear stress

WSS is a time-resolved three-dimensional force that was calculated from the 4D-CMR data set using a dedicated software tool based on Matlab® (The MathWorks, Natick, MA, USA) as previously described.[17] Three different WSS vectors were calculated: axial, circumferential, and magnitudinal (*Figure 4*). Axial WSS (WSS_{axial}) is the dominating vector of WSS in laminar flow and is perpendicular to an axial slice through the vessel and parallel to the direction of flow. Circumferential WSS (WSS_{circ}) is the dominating vector of WSS in a helical flow and is parallel to the vessel wall circumference. Magnitudinal WSS (WSS_{mag}) as a time-resolved vector quantity that can be

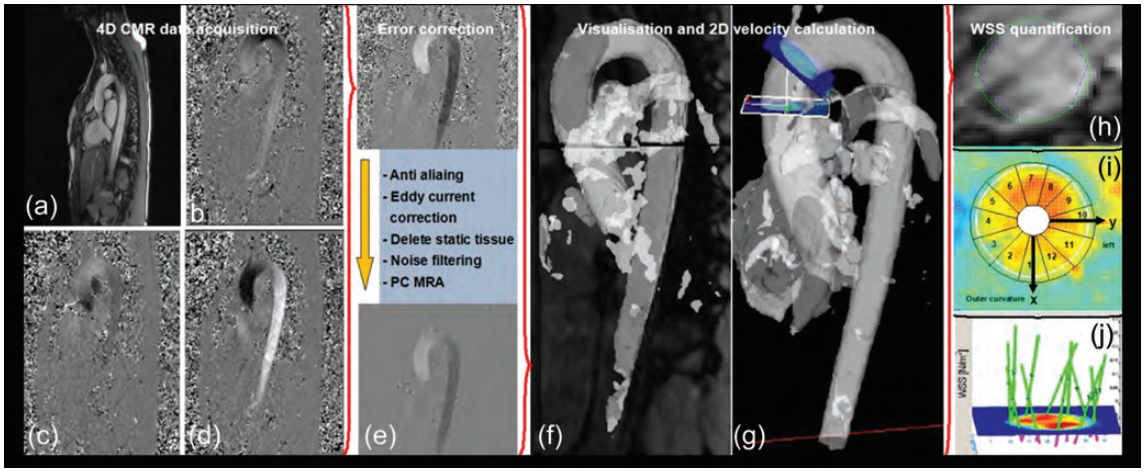

Figure 1 4D-CMR data acquisition and WSS quantification. Work flow of 4D-CMR data acquisition, pre-processing, and WSS quantification; (*a*) magnitude image; (*b*) phase-contrast image *x*-axis; (*c*) phase-contrast image *y*-axis; (*d*) phase-contrast image z-axis; (e) post-processing with anti-aliasing, eddy-current correction, static tissue deletion, noise filtering and time-independent phase-contrast-MR-angiography (PC-MRA); (*f* and *g*) landmark positioning in the ascending aorta; (*h*) definition of the region of interest for WSS quantification; (*i*) definition of vessel orientation and segmental analysis; (*j*) the green bars show the visualization of WSS. EnSight® and dedicated software tools based on MATLAB® were used.

characterized by its magnitude is the resulting net vector along the entire vascular wall (*Figure 4*).[17,25]

Orthogonal square 2D planes were manually positioned along the 3D data sets of the ascending aorta at pre-defined landmarks. These landmarks were the mid-ascending aorta at the level of the bifurcation of the main pulmonary artery (MPA level) and the distal ascending aorta at the level just before the branching of the brachiocephalic trunk (BCT level) (*Figure 1*). The derived data from these planes encoded 4D-CMR data as well as 2D planar information of velocity and vessel wall parameters. WSS_{axial}, WSS_{circ}, and WSS_{mag} at the vessel wall were calculated over one cardiac cycle for each vessel wall segment as previously described (*Figure 5*).[17]

Statistical analysis

Data analysis was performed using StatView® (StatView®, SAS Institute, Cary, version 5.0.1). For statistical analysis, the Wilcoxon signed-rank test and the Mann–Whitney *U* test were used. A *P*-value ≤ 0.05 was considered to be significant.

Results

Bicuspid aortic valve study group

Eighteen individuals (eight females) with congenital BAV (without cardiovascular disease) were prospectively recruited for this study. Valve morphology was evaluated and confirmed during the CMR study by cine studies. These 18 individuals were median 25 (range 10–44) years old, had a median body height of 177 (range 138–192) cm, a body weight of median 68 (range 30–94) kg, a systolic blood pressure of median 109 (range 98–128) mmHg, a diastolic blood pressure of median 65 (range 46–83) mmHg, a velocity through the aortic valve of median 1.4 m/s (range 1.1–2.3), and a regurgitation fraction through the aortic valve of 1% (range 0–7%). The diameter of the ascending aorta was median 1.62 cm/m^2 (range 1.14–2.26 cm/m^2).

Tricuspid aortic valve study group

These 18 individuals were median 25 (range 8–42) years old, had a median body height of 174 (range 130–188) cm, a body weight of median 68 (range 29–95) kg, a systolic blood pressure of median 107 (range 94–122) mmHg, a diastolic blood pressure of median 58 (range 47–82) mmHg, a velocity through the aortic valve of median 1.1 m/s (range 0.9–1.7), and a regurgitation fraction through the aortic valve of 0% (range 0–4%). The diameter of the ascending aorta was median 1.32 cm/m^2 (range 1.05–1.68 cm/m^2).

There was no significant difference in sex, age, body height, body weight, systolic, or diastolic blood pressure between the two groups.

Aortic valve morphology

Evaluation of the BAV morphology yielded in two patterns. Thirteen of 18 patients (72%) with BAV were identified as BAV type 1 with fusion of the right and left coronary cusp, the remaining five (28%) as BAV type 2 with fusion of the right and non-coronary cusp.

Blood flow pattern

The analysis of the flow patterns in individuals with BAV and TAV showed a significant association between a helical flow and the presence of BAV. (*Figure 2*) The classification into the Grades 0–3 according to the degree of abnormal helical flow patterns was significantly different in the matched pairs ($P = 0.0004$). In the BAV group, 85% of the flow patterns were classified as

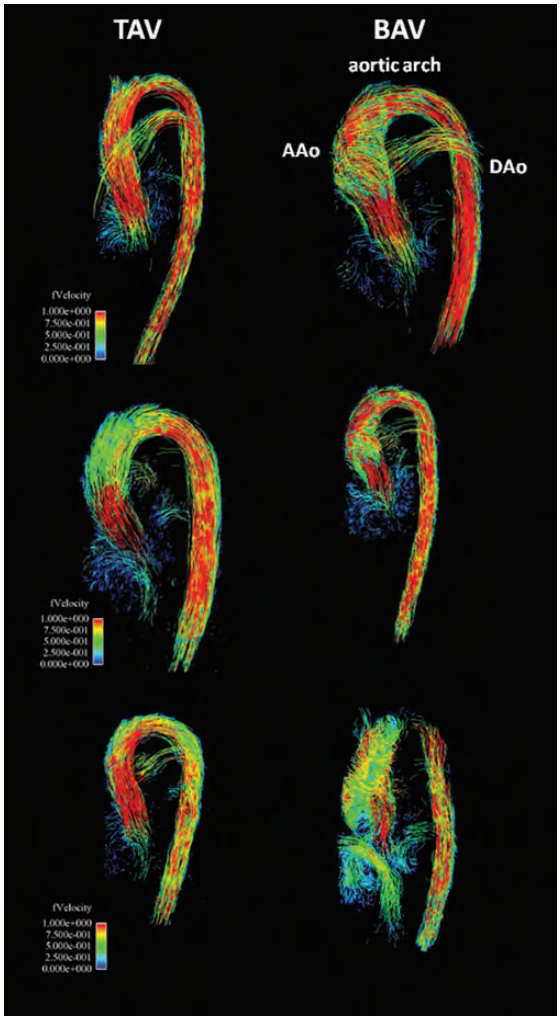

Figure 2 Flow patterns in the ascending aorta. Flow pattern in the ascending aorta in three matched pairs are shown (particle traces). Control persons on the left side and individuals with BAV on the right side. In BAV patients, the helical flow patterns are shown. Ascending aorta (AAo); descending aorta (DAo).

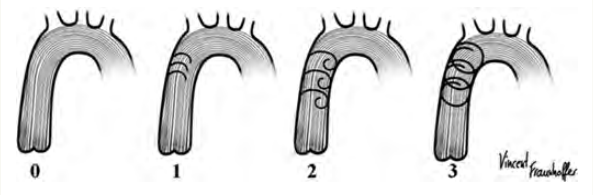

Figure 3 Classification of flow patterns. Grade 0 was defined as a linear flow in the ascending aorta, Grade 1 as a helical flow $<180^{\circ}$, Grade 2 as a helical flow of $180-360^{\circ}$, and Grade 3 as a helical flow $>360^{\circ}$.

Grade 2 or 3. In the TAV group, 94% of the flow patterns were graded as 0 or 1. (*Figure 6*)

Comparing the individuals with BAV type 1 ($n = 13$) and type 2 ($n = 5$), none of the individuals with BAV type 2 was classified as

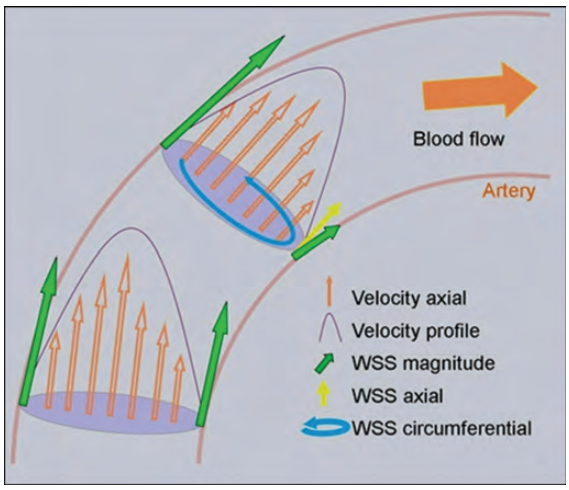

Figure 4 Different wall shear stress patterns. Illustration of the different wall shear stress (WSS) patterns at the aortic wall. WSSaxial, WSScircumferential, and WSSmagnitude are shown.

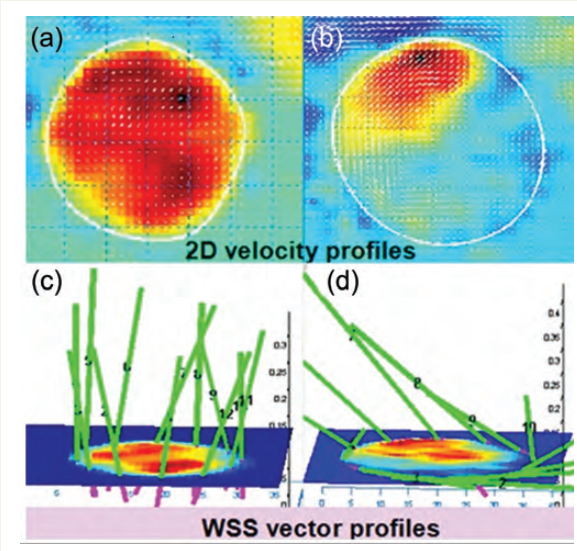

Figure 5 Flow and WSS quantification in the mid-ascending aorta. Results of flow and WSS quantification in the mid-ascending aorta in two 32-year-old women. (*a* and *c*) TAV; (*b* and *d*) BAV; the upper panel on each side shows the 2D velocity profiles with the unequally distributed flow field in BAV. The green bars in the lower panel present WSS_{mag} over the entire cardiac cycle. The bars visualize the amount of the WSS_{mag} on the vessel wall.

Grade 0 or 1 by the three observers (15 observations), but classified Grade 2 twice and Grade 3 thirteen times. In contrast, in the subgroup of type 1 leaflet morphology Grade 0 was classified five times, Grade 1 three times, Grade 2 six times, and Grade 3 twenty-five times by three observers (39 observations).

Two individuals of the BAV type II showed left-handed helical flow patterns, the other three individuals with BAV type II, and all BAV type I individuals showed right-handed flow patterns.

Wall shear stress

Axial, circumferential, and WSS_{mag} were significantly abnormal in the mid-ascending aorta at the level of the MPA in the BAV study group compared with the TAV control group (*Figure 7*). Whereas WSS_{axial} was significantly decreased in the BAV study group compared with the TAV control group, WSS_{circ} and WSS_{mag} were both significantly increased. In the distal ascending aorta at the level just before the branching of the BCT, only WSS_{circ} was significantly increased in the BAV study group compared with the TAV control group. WSS_{axial} and WSS_{mag} were not altered (*Table 1*).

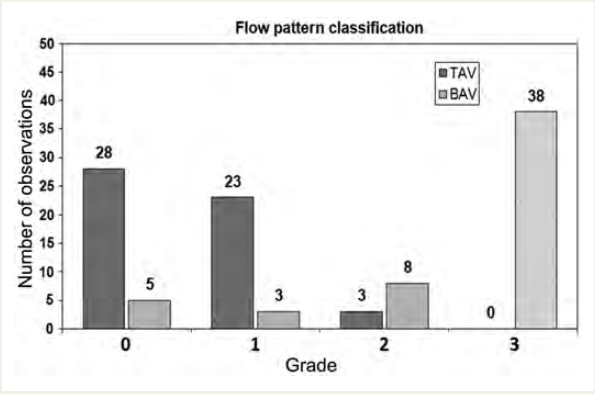

Figure 6 Grading of a helical flow pattern in the ascending aorta. Grading of the flow scenarios of 36 individuals with BAV or TAV by three blinded investigators ($n = 108$).

Discussion

This prospectively designed study showed significantly altered flow patterns and WSS in the ascending aorta of individuals with BAV compared with age- and sex-matched individuals with TAV. Eighty-five per cent of the individuals with BAV had a severe helical flow pattern in the ascending aorta. In contrast, 94% of the individuals with TAV had a laminar flow pattern and none had a highly severe helical flow pattern in the ascending aorta.

It is important to note, that none of the individuals in this study had moderate to severe aortic stenosis or moderate to severe aortic valve regurgitation or other cardiovascular disease.

This study shows that the cumulative net WSS (WSS_{mag}) and WSS_{circ} were significantly increased in individuals with BAV compared with individuals with TAV in the mid-ascending aorta (MPA level). (*Figure 7*) On the other hand, WSS_{axial} was significantly decreased in individuals with BAV compared with individuals with TAV at the mid-ascending aorta. These large significant alterations in WSS occurred at the mid-ascending aorta, the level where dilation in individuals with BAV mainly occurs.[27] Further downstream, in the distal ascending aorta (BCT level) we found the same findings, although less extreme. Putting the flow and WSS results together, we conclude, that in individuals with TAV predominant laminar flow leads to a predominant WSS_{axial}, whereas WSS_{circ} is usually nearly zero. In contrast, in individuals with BAV

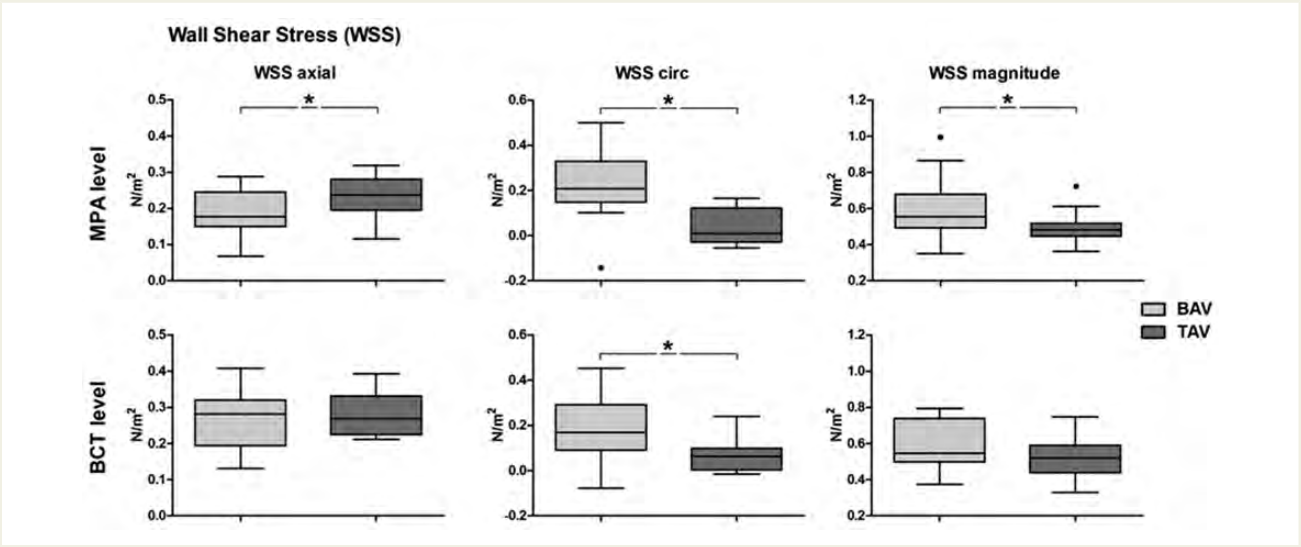

Figure 7 Wall shear stress in the ascending aorta. Boxplot graphs (Tukey): WSS_{axial}, WSS_{circ}, and WSS_{mag} measured in the mid-ascending aorta at the level of the main pulmonary artery (MPA level; upper panels) and at the level of the distal ascending aorta just before the branching of the brachiocephalic trunk (BCT level; lower panels); WSS_{axial} at the MPA level was significantly decreased in the BAV study group compared with the TAV control group. WSS_{axial} at the BCT level showed no significant differences. WSS_{circ} at MPA and at BCT level were significantly increased in the BAV study group compared with the TAV control group. WSS_{mag} at the MPA level was significantly increased in the BAV study group compared with the TAV control group. WSS_{mag} at the BCT level showed no significant differences.

Table 1 Wall shear stress in the ascending aorta

	BAV		TAV		*P*-value
	WSS median (N/m^2)	range	WSS median (N/m^2)	range	
WSS_{axial}					
MPA level	0.18	0.07 to 0.29	0.24	0.12 to 0.32	0.007
BCT level	0.28	0.13 to 0.41	0.27	0.21 to 0.39	0.420
WSS_{circ}					
MPA level	0.21	−0.14 to 0.50	0.01	−0.05 to 0.17	0.014
BCT level	0.17	−0.08 to 0.45	0.06	−0.01 to 0.24	0.008
WSS_{mag}					
MPA level	0.55	0.35 to 1.00	0.48	0.36 to 0.72	0.028
BCT level	0.55	0.37 to 0.79	0.52	0.33 to 0.75	0.145

MPA level, ascending aorta at the level of the main pulmonary artery; BCT level, distal ascending aorta before the branching of the brachiocephalic trunk.

predominant helical flow reduces WSS_{axial} and causes a significantly higher WSS_{circ}, resulting in increased cumulative net WSS (WSS_{mag}). These alterations may be the cause of aortic dilation in individuals with BAV.

The influence of haemodynamic shear stress due to spatial and temporal alterations in shear forces on the endothelium has been described by others showing regionally different flow and arterial remodelling. The mechanical shear forces induced by the blood flow seem to play an important role in the process of vascular remodelling.[17,28] Altered flow characteristics with regionally varying WSS has been demonstrated by Frydrychowicz *et al.*[21,29] showing the correlation of WSS with the development of high-risk plaques in the carotid arteries and selected pathologies.

Different shear forces act on the vessel wall. They may act along the axial and circumferential direction. The effective WSS has to be considered as a vector quantity from axial and circumferential components.[17,30]

Helical flow patterns have already been described in patients with BAV and additional cardiovascular disease such as aortic stenosis, aortic regurgitation, coarctation of the aorta, or tetralogy of Fallot.[16] In a retrospective evaluation of patients studied by 4D–CMR, Hope *et al.*[31] described asymmetrically distributed WSS in BAV and eccentric systolic blood flow, postulating increased haemodynamic burden in BAV as a risk for aneurysm formation in the ascending aorta. In a recently published study of Barker *et al.*,[32] they described altered WSS in the ascending aorta in BAV disease, but most of the subjects in the BAV study population had aortic aneurysms or concomitant aortic stenosis or regurgitation.

In this prospective study, it was possible to measure and calculate *in vivo* data of WSS in individuals with pure BAV disease by 4D-CMR. Therefore, we compared healthy individuals with BAV that were matched by age and sex with healthy control individuals with TAV. Very strict inclusion criteria ruled out any individual with an additional co-morbidity. A further strength of this study might be the matched-pair character, since such a homogeneous group has not been described so far.

A recent, well designed, study concluded that the risk of dilation, dissection, or rupture of the ascending aorta still cannot be estimated for individuals with BAV using established simple clinical criteria based on aortic diameters.[5] The authors furthermore demanded that 'research efforts should concentrate on (. . .) identifying nonsize markers for refining risk prediction of aortic dissection in these patients'.[5] We suggest that helical flow patterns and WSS_{circ} in the ascending aorta might be such a non-size marker. Interestingly, 15% of the individuals with BAV in our study did not have helical flow patterns in the ascending aorta. It might be possible that these individuals may have a lower risk than the other 85% of the individuals with BAV in this study population. Follow-up studies may help to evaluate the course of aortic enlargement and the development of altered flow patterns during life. This might help to distinguish patients at risk for aortic dilatation.

According to the leaflet morphology, it was remarkable that all of our evaluations of BAV type 2 showed a severe helical flow. These findings are consistent with a previously described distribution, evaluating different patterns of aortic elasticity, and aortic root shape comparing different BAV types.[33] It has been suggested that differences in a spatial distribution of the blood flow through the different valve patterns may lead to an inhomogeneous distribution of shear forces, resulting in differential gene expression and changes of the extra cellular matrix.[33] Different flow patterns may lead to altered distribution of WSS patterns and this may lead to changes of aortic wall properties. In this manner, BAV type 2 is commonly associated with more severe valve pathologies especially aortic valve stenosis.[34] We tried to distinguish important differences in the flow for these two phenotypes, but our study subgroups for BAV type 1 and 2 were too small to answer specific leaflet dependent questions in a statistically reliable way.

An association between BAV and cystic media necrosis has been described based on observations in four cases.[35] In a case report of a father and a son, it was suggested that changes in the media of the vessels occur due to a developmental defect.[36] In contrast, cystic media necrosis may also occur as a secondary effect due to an ischaemic or distended aortic wall.[37,38]

Others did not find an association of BAV stenosis or regurgitation with aortic dilatation.[8,9,11] In a mixed group of patients with

BAV, coarctation of the aorta, and TAV an increased incidence of cystic media necrosis was found in patients with BAV without an association with dilatation.[14] These groups concluded that their results support the theory of an underlying developmental defect. However, a missing association does not prove a competing theory. We found significantly altered flow pattern and WSS in individuals with BAV without aortic valve stenosis or regurgitation, aortic dilatation, or coarctation of the aorta. Therefore, in our view, there is a clear association of BAV and altered flow and WSS. Aortic dilation may be explained by the hypothesis that BAV generates a helical flow pattern in the ascending aorta and increases WSS with possible consecutive aortic wall remodelling. The altered aortic wall properties may further lead to dilation. Whether these altered flow patterns and WSS lead to aortic dilation remains to be elucidated. A limitation of our study is that due to the study design we could not examine histological alterations in the aortic wall of these individuals.

In conclusion, despite a tremendous amount of studies about dilation in BAV, there is no proven evidence of an inborn tissue disorder leading to aortic dilation. In this prospective study, we could demonstrate pathological flow patterns and increased WSS in the ascending aorta in healthy BAV individuals without concomitant valvular lesions and with normal aortic diameters. Possibly, the characterization of blood flow patterns may help as a non-size marker to select and follow-up patients with BAV at risk for aortic dilation in future.

Acknowledgement

We thank Vincent Fraunhoffer for graphical art design of *Figure 3*.

Ethics approval

This prospective study was approved by the faculty's ethical board. Written informed consent was obtained from all participants or their parents. No participant received financial support.

Conflict of interest: none declared.

References

1. Siu SC, Silversides CK. Bicuspid aortic valve disease. *J Am Coll Cardiol* 2010;**55**:2789–2800.
2. Roberts WC. The congenitally bicuspid aortic valve. A study of 85 autopsy cases. *Am J Cardiol* 1970;**26**:72–83.
3. Fedak PWM, Verma S, David TE, Leask RL, Weisel RD, Butany J. Clinical and pathophysiological implications of a bicuspid aortic valve. *Circulation* 2002;**106**:900–4.
4. Bonow RO. Bicuspid aortic valves and dilated aortas: a critical review of the ACC/AHA practice guidelines recommendations. *Am J Cardiol* 2008;**102**:111–4.
5. Michelena HI, Khanna AD, Mahoney D, Margaryan E, Topilsky Y, Suri RM *et al.* Incidence of aortic complications in patients with bicuspid aortic valves. *JAMA* 2011;**306**:1104–12.
6. Mahle WT, Sutherland JL, Frias PA. Outcome of isolated bicuspid aortic valve in childhood. *J Pediatr* 2010;**157**:445–9.
7. Nistri S, Sorbo MD, Marin M, Palisi M, Scognamiglio R, Thiene G. Aortic root dilatation in young men with normally functioning bicuspid aortic valves. *Heart* 1999;**82**:19–22.
8. Hahn RT, Roman MJ, Mogtader AH, Devereux RB. Association of aortic dilation with regurgitant, stenotic and functionally normal bicuspid aortic valves. *J Am Coll Cardiol* 1992;**19**:283–8.
9. Keane MG, Wiegers SE, Plappert T, Pochettino A, Bavaria JE, Sutton MG. Bicuspid aortic valves are associated with aortic dilatation out of proportion to coexistent valvular lesions. *Circulation* 2000;**102**:III35–9.
10. Roberts CS, Roberts WC. Dissection of the aorta associated with congenital malformation of the aortic valve. *J Am Coll Cardiol* 1991;**17**:712–6.
11. Pachulski RT, Weinberg AL, Chan KL. Aortic aneurysm in patients with functionally normal or minimally stenotic bicuspid aortic valve. *Am J Cardiol* 1991;**67**:781–2.
12. den Reijer PM, Sallee D, van der Velden P, Zaaijer ER, Parks WJ, Ramamurthy S *et al.* Hemodynamic predictors of aortic dilatation in bicuspid aortic valve by velocity-encoded cardiovascular magnetic resonance. *J Cardiovasc Magn Reson* 2010;**12**:4.
13. Guntheroth WG. A critical review of the American College of Cardiology/American Heart Association practice guidelines on bicuspid aortic valve with dilated ascending aorta. *Am J Cardiol* 2008;**102**:107–10.
14. Bonderman D, Gharehbaghi-Schnell E, Wollenek G, Maurer G, Baumgartner H, Lang IM. Mechanisms underlying aortic dilatation in congenital aortic valve malformation. *Circulation* 1999;**99**:2138–43.
15. Hope TA, Markl M, Wigström L, Alley MT, Miller DC, Herfkens RJ. Comparison of flow patterns in ascending aortic aneurysms and volunteers using four-dimensional magnetic resonance velocity mapping. *J Magn Reson Imaging* 2007;**26**:1471–9.
16. Hope MD, Hope TA, Meadows AK, Ordovas KG, Urbania TH, Alley MT *et al.* Bicuspid aortic valve: four-dimensional MR evaluation of ascending aortic systolic flow patterns. *Radiology* 2010;**255**:53–61.
17. Frydrychowicz A, Stalder AF, Russe MF, Bock J, Bauer S, Harloff A *et al.* Three-dimensional analysis of segmental wall shear stress in the aorta by flow-sensitive four-dimensional-MRI. *J Magn Reson Imaging* 2009;**30**:77–84.
18. Markl M, Harloff A, Bley TA, Zaitsev M, Jung B, Weigang E *et al.* Time-resolved 3D MR velocity mapping at 3T: improved navigator-gated assessment of vascular anatomy and blood flow. *J Magn Reson Imaging* 2007;**25**:824–31.
19. Markl M, Chan FP, Alley MT, Wedding KL, Draney MT, Elkins CJ *et al.* Time-resolved three-dimensional phase-contrast MRI. *J Magn Reson Imaging* 2003;**17**:499–506.
20. Markl M, Draney MT, Hope MD, Levin JM, Chan FP, Alley MT *et al.* Time-resolved 3-dimensional velocity mapping in the thoracic aorta: visualization of 3-directional blood flow patterns in healthy volunteers and patients. *J Comput Assist Tomogr* 2004;**28**:459–68.
21. Frydrychowicz A, Berger A, Russe MF, Stalder AF, Harloff A, Dittrich S *et al.* Time-resolved magnetic resonance angiography and flow-sensitive 4-dimensional magnetic resonance imaging at 3 Tesla for blood flow and wall shear stress analysis. *J Thorac Cardiovasc Surg* 2008;**136**:400–7.
22. Frydrychowicz A, Markl M, Harloff A, Stalder AF, Bock J, Bley TA *et al.* Flow-sensitive *in vivo* 4D MR imaging at 3T for the analysis of aortic hemodynamics and derived vessel wall parameters. *Rofo* 2007;**179**:463–72.
23. Bonow RO, Carabello BA, Chatterjee K, de Leon AC, Faxon DP, Freed MD *et al.* 2008 focused update incorporated into the ACC/AHA 2006 guidelines for the management of patients with valvular heart disease: a report of the American College of Cardiology/American Heart Association Task Force on Practice Guidelines (Writing Committee to revise the 1998 guidelines for the management of patients with valvular heart disease). Endorsed by the Society of Cardiovascular Anesthesiologists, Society for Cardiovascular Angiography and Interventions, and Society of Thoracic Surgeons. *J Am Coll Cardiol* 2008;**52**:e1–142.
24. Schaefer BM, Lewin MB, Stout KK, Gill E, Prueitt A, Byers PH *et al.* The bicuspid aortic valve: an integrated phenotypic classification of leaflet morphology and aortic root shape. *Heart* 2008;**94**:1634–8.
25. Stalder AF, Russe MF, Frydrychowicz A, Bock J, Hennig J, Markl M. Quantitative 2D and 3D phase contrast MRI: optimized analysis of blood flow and vessel wall parameters. *Magn Reson Med* 2008;**60**:1218–31.
26. Napel S, Lee DH, Frayne R, Rutt BK. Visualizing three-dimensional flow with simulated streamlines and three-dimensional phase-contrast MR imaging. *J Magn Reson Imaging* 1992;**2**:143–53.
27. Bauer M, Gliech V, Siniawski H, Hetzer R. Configuration of the ascending aorta in patients with bicuspid and tricuspid aortic valve disease undergoing aortic valve replacement with or without reduction aortoplasty. *J Heart Valve Dis* 2006;**15**:594–600.
28. Davies PF. Flow-mediated endothelial mechanotransduction. *Physiol Rev* 1995;**75**:519–60.
29. Frydrychowicz A, Arnold R, Hirtler D, Schlensak C, Stalder AF, Hennig J *et al.* Multidirectional flow analysis by cardiovascular magnetic resonance in aneurysm development following repair of aortic coarctation. *J Cardiovasc Magn Reson* 2008;**10**:30.
30. Ku DN, Giddens DP, Zarins CK, Glagov S. Pulsatile flow and atherosclerosis in the human carotid bifurcation. Positive correlation between plaque location and low oscillating shear stress. *Arteriosclerosis* 1985;**5**:293–302.

31. Hope MD, Hope TA, Crook SES, Ordovas KG, Urbania TH, Alley MT *et al.* 4D flow CMR in assessment of valve-related ascending aortic disease. *JACC Cardiovasc Imaging* 2011;**4**:781–7.
32. Barker AJ, Markl M, Burk J, Lorenz R, Bock J, Bauer S *et al.* Bicuspid aortic valve is associated with altered wall shear stress in the ascending aorta. *Circ Cardiovasc Imaging* 2012;**5**:457–66.
33. Schaefer BM, Lewin MB, Stout KK, Byers PH, Otto CM. Usefulness of bicuspid aortic valve phenotype to predict elastic properties of the ascending aorta. *Am J Cardiol* 2007;**99**:686–90.
34. Fernandes SM, Sanders SP, Khairy P, Jenkins KJ, Gauvreau K, Lang P *et al.* Morphology of bicuspid aortic valve in children and adolescents. *J Am Coll Cardiol* 2004;**44**:1648–51.
35. McKusick VA, Logue RB, Bahnson HT. Association of aortic valvular disease and cystic medial necrosis of the ascending aorta: report of four instances. *Circulation* 1957;**16**:188–94.
36. McKusick VA. Association of congenital bicuspid aortic valve and Erdheim's cystic medial necrosis. *Lancet* 1972;**1**:1026–7.
37. Stefanadis C, Vlachopoulos C, Karayannacos P, Boudoulas H, Stratos C, Filippides T *et al.* Effect of vasa vasorum flow on structure and function of the aorta in experimental animals. *Circulation* 1995;**91**:2669–78.
38. Stefanadis CI, Karayannacos PE, Boudoulas HK, Stratos CG, Vlachopoulos CV, Dontas IA *et al.* Medial necrosis and acute alterations in aortic distensibility following removal of the vasa vasorum of canine ascending aorta. *Cardiovasc Res* 1993;**27**:951–6.

IMAGE FOCUS

doi:10.1093/ehjci/jet035
Online publish-ahead-of-print 14 March 2013

Rheumatic disease mimicking an infiltrative mass of the mitral valve

Ferande Peters[1], Bijoy K. Khandheria[2]*, Michelle L. Wong[3], and Mohammed R. Essop[1]

[1]Department of Cardiology, Chris Hani Baragwanath Hospital, University of the Witwatersrand, Diepkloof 319-Iq, Johannesburg, Soweto 1862, South Africa; [2]Aurora Cardiovascular Services, Aurora Sinai/Aurora St Luke's Medical Centers, University of Wisconsin School of Medicine and Public Health, 2801 W. Kinnickinnic River Parkway, #840, Milwaukee, WI 53215, USA; and [3]Department of Pulmonology, Chris Hani Baragwanath Hospital, University of the Witwatersrand, Diepkloof 319-Iq, Johannesburg, Soweto 1862, South Africa

* Corresponding author. Tel: +1 414 649 3909; fax: +1 414 649 3551. Email: publishing22@aurora.org

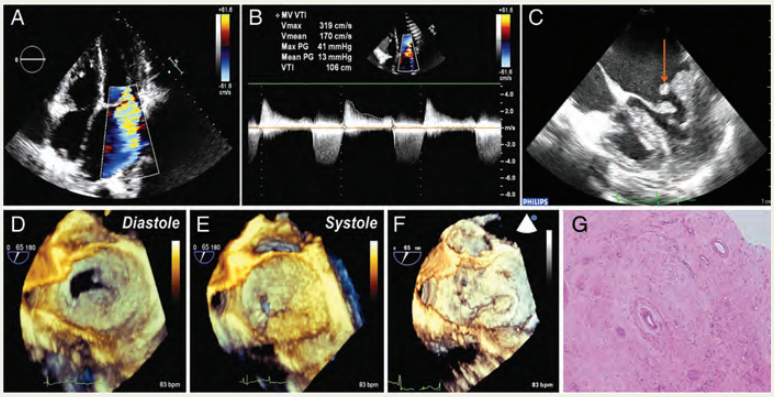

A 32-year-old man previously was diagnosed with sarcoidosis on the basis of bilateral lung infiltrates, hypercalcaemia, multiple renal calculi and an elevated serum angiotensin-converting enzyme level, all of which improved on corticosteroids. Nine months later he developed symptomatic, sputum-positive pulmonary tuberculosis and tuberculous lymphadenitis, which were successfully treated.

At his initial presentation, there was evidence of severe mitral regurgitation and moderate mitral stenosis complicated by severe pulmonary hypertension (*Panels A* and *B*).The medial halves of both mitral leaflets were immobilized by what appeared to be an infiltrative process with an associated pedunculated mass (*Panels C–F*, see Supplementary data online, *Videos S1* and *S2*). The subvalvular apparatus and basal posterior wall were abnormal and presumed to represent a continuum of the infiltrative process. No clinical or laboratory features of infective endocarditis were present. Two years later, the morphology of the valve was unchanged except for the absence of the pedunculated mass, while the degree of pulmonary hypertension and mitral stenosis was worse. Cardiac catheterization confirmed the severe pulmonary hypertension was due almost exclusively to the severe mixed mitral valve disease. This haemodynamic abnormality was eliminated following successful mitral valve replacement.

Histology of the resected valve revealed features of chronic inflammation compatible with chronic rheumatic disease with no features suggestive of tuberculosis or sarcoid (*Panel G*). We postulate that the pedunculated mass might have represented nonbacterial endocarditis and that excessive scarring and chronic inflammation from untreated rheumatic disease resulted in this unusual morphological appearance of the mitral valve.

Supplementary data are available at *European Heart Journal – Cardiovascular Imaging* online.